

DOI: 10.21767/2572-4657.100007

## FT-IR, FT-Raman and UV-Visible Spectral Analysis on (E)-N'-(thiophen-2-ylmethylene) Nicotinothiazide

**Bharanidharan S<sup>1</sup>,  
Saleem H<sup>1</sup>,  
Subashchandrabose S<sup>2</sup>,  
Suresh M<sup>3</sup> and  
Ramesh Babu N<sup>4</sup>**

### Abstract

Vibrational analysis of the (E)-N'-(thiophen-2-ylmethylene) nicotinothiazide (T2CNH) compound was carried out in solid phase using FTIR and FT-Raman spectroscopic techniques in the ranges: 400-4000 cm<sup>-1</sup> and 100-4000 cm<sup>-1</sup>, respectively. The molecular geometries and harmonic vibrational frequencies were calculated using DFT/6-311++G(d,p) basis set. A detailed interpretation of the IR and Raman spectra, based on the total energy distribution (TED) of the normal modes. The bond parameters such as bond lengths, bond angles and dihedral angles were calculated at the same level of theory. The natural bonding orbital (NBO) study reveals that inter and intra-molecular charge transfer of the molecule. The electronic transition was studied using UV-Vis spectrum. The NLO, band gap energy, MEP map, Mulliken atomic charges were calculated using the same level of basis set. In addition the thermodynamic properties were also calculated.

**Keywords:** FT-IR; FT-Raman; TED; NBO; T2CNH

- 1 Department of Physics, Annamalai University, Annamalainagar-608002, Tamil Nadu, India
- 2 Centre for Research and Development, PRIST University, Thanjavur-613403, Tamil Nadu, India
- 3 Department of Chemistry, College of Engineering, Guindy, Anna University, Chennai, 620 025, India
- 4 Dept. of Physics, M.I.E.T. Engineering College, Trichy-620007, Tamil Nadu, India

**Corresponding author:** Saleem H

✉ saleem\_h2001@yahoo.com

**Received:** December 21, 2016; **Accepted:** January 02, 2017; **Published:** January 09, 2017

Department of Physics, Annamalai University, Tamil Nadu, India.

**Tel:** +91 9443879295

### Introduction

Generally, Pyridine ring is a heterocyclic organic compound with the chemical formula C<sub>5</sub>H<sub>5</sub>N. Pyridine is structurally related to benzene, with one methine group (=CH-) replaced by a nitrogen atom. It occurs in many important compounds, including azines and the vitamins niacin and pyridoxal. The precursor of pyridine is used to agrochemicals, pharmaceuticals and is also an important solvent and reagent. Mostly, it is used in the *in vitro* synthesis of DNA, sulfa pyridine (a drug against bacterial and viral infections), antihistaminic drugs tripeleminamine and mepyramine, as well as water repellents, bactericides, and herbicides. Some chemical compounds, although not synthesized from pyridine, contain its ring structure. They include B vitamins niacin and pyridoxal, an anti-tuberculosis drug isoniazide, nicotine and other nitrogen-containing plant products [1].

The ring of Thiophene and its derivatives have been reported to possess broad spectrum of biological properties including anti-inflammatory, analgesic, antidepressant, antimicrobial and anticonvulsant activities [2-4]. Antiepileptic drugs (AEDs) like tiagabine, etizolam, brotizolam are containing thiophene moiety

in their structures as active pharmacophore [5,6]. In addition, thiophene and its derivatives functionalized with the formyl group are versatile building blocks for the synthesis of donor-acceptor substituted p-conjugated systems for several optical applications.

The hydrazone group in the organic compound brings out several physical and chemical properties. The hydrazones are bearing the >C=N-N< which leads the molecule towards nucleophilic and electrophilic in nature. In the hydrazone moiety, the nitrogen atom behaves as nucleophilic and carbon atom behaves as nucleophilic as well as electrophilic in nature [7-9]. The benzohydrazone derivatives shows wide spectrum of

biological activities such as antibacterial [10], antifungal [11] and antitubercular [12] activities.

Subashchandrabose et al. [13] recorded the FT-IR, FT-Raman and UV-Vis spectra for the molecule N1-N2-bis((pyridine-4-yl)methylene)benzene-1,2-diamine. The observed FT-IR and FT-Raman spectral values were compared with the calculated wave numbers. For the prediction of accurate vibrational assignments TED analysis was performed using SQM method. The bond lengths and bond angles of stable conformer were correlated well with the experimental values. The hyperconjugative interaction and charge delocalization around the bonds were studied using NBO analysis. Band gap energy was also determined.

Quantum chemical calculations of energies, geometrical structure and vibrational wavenumber of 1,2-bis(3-methoxy-4-hydroxybenzylidene)hydrazine were carried out by Subramanian et al. [14] using DFT method with 6-31G(d) as basis set. The optimized geometrical parameters obtained by DFT calculations are in good agreement with single crystal XRD data. The vibrational spectral data were obtained from FT-IR and FT-Raman spectra are assigned based on the results of the theoretical calculations in solid phase.

From Literature survey reveals that the vibrational analysis of (E)-N'-(thiophen-2-ylmethylene) nicotinohydrazide (T2CNH) has not yet been reported. The T2CNH molecule was synthesized and its structural characterization was calculated by B3LYP/6-311++G(d,p) basis set. The spectral investigation such as FT-IR, FT-Raman and UV-Vis spectra were recorded. The observed spectral results were compared with the computed wavenumber. The vibrational assignments of the title molecule were carried out with the help of TED. The First order hyperpolarizability, Homo-Lumo energy gap was calculated and furthermore, the MEP and thermodynamic properties were also calculated.

## Computational Details

The entire theoretical calculations were performed DFT method at B3LYP/6-311++G(d,p) basis set to using Gaussian 03W [15] program package, invoking gradient geometry optimization [15,16]. The geometrical parameters were used in the vibrational frequency calculations at the same level to characterize all the stationary points as minima. The vibrationally averaged nuclear positions of T2CNH were used for harmonic vibrational frequency calculations resulting in IR and Raman frequencies together with intensities and Raman depolarization ratios. The vibrational modes were assigned on the basis of TED analysis using VEDA4 program package [17]. The Raman activity was calculated by using Gaussian 03W package and the activity was transformed into Raman intensity using Raint program [18] by the expression:

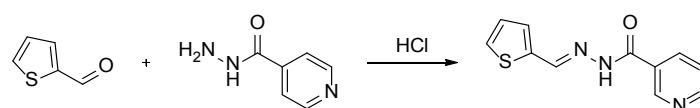
$$I_i = 10^{-12} \times (v_o - v_i)^4 \times \frac{1}{v_i} \times R A_i \quad (1)$$

Where  $I_i$  is the Raman intensity,  $R A_i$  is the Raman scattering activities,  $v_i$  is the wavenumber of the normal modes and  $v_o$  denotes the wavenumber of the excitation laser [19].

## Experimental Details

### Synthesis procedure

A mixture of Thiophene-2-carboxaldehyde (2.1 mL, 0.01 mol) and nicotinic acid hydrazide (1.37 g, 0.01 mol) in 5 mL of ethanol was stirred in the presence of 2 drops of concentrated HCl for one hour. The reaction mixture was maintained at room temperature and the colourless solid was obtained. The solid was separated and filtered under suction, washed with ice-cold water (50 ml). The precipitate was washed with water and filtered and again washed with petroleum ether (40-60%) and dried over in a vacuum desiccator then the product was recrystallized from hot ethanol.



## Results and Discussion

### Molecular Geometry

The T2CNH molecule was optimized by B3LYP/6-311++G(d,p) level of basis set. This molecule consists of thiophene and pyridine rings are fused by hydrazone linkage. The calculated bond length of  $C_2-S_1$  is expected to be shorter than the  $C_5-S_1$  bond length, since the hydrozone moiety is attached with  $C_2$  atom and their corresponding bond distances are 1.750 and 1.728Å. The bond lengths of  $C_2=C_3$ ,  $C_3-C_4$ ,  $C_4=C_5$  are 1.377, 1.418, 1.369Å and the bond angles of  $C_2-C_3-C_4$ ,  $C_3-C_4-C_5$  are 113.02°, 113.03°. The bond angles  $S_1-C_2-C_3$  and  $S_1-C_5-C_4$  are differ by ~1° which is due to the shortening of bond distance between  $S_1$  and  $C_2$  atoms. These values are particularly in good agreement with the values of anti thiophen-2-aldehyde [20] and thiophen-2-carbohydrazide [21]. Furthermore, these values are also find support from literature [22]. The dihedral angles of  $S_1-C_2-C_9-N_{11}/S_1-C_2-C_9-H_{10}$  and  $C_3-C_2-C_9-N_{11}/C_3-C_2-C_9-H_{10}$  are -179.96°/-0.07° and 0.03°/+179.93°, respectively, which shows that the thiophen and hydrozone moieties of T2CNH are co-planar. Since there is a good conjugation between p-orbitals of all atoms of thiophen and hydrazone moieties. Most of the calculated geometrical parameters are find support from single crystal X-ray diffraction values [23,24]. It should be mentioned that there is no significant difference between the geometrical parameters of the hydrozone and pyridine moieties [23,24]. The geometrical parameters and optimized structure of the T2CNH molecule are presented in **Table 1** and **Figure 1**, respectively.

### Vibrational Assignments

The T2CNH molecule belongs to  $C_1$  point group symmetry. It consists of 25 atoms which undergoes 69 normal modes of vibrations. In which 47 modes of vibrations are in-plane and 22 are out-of-plane bending vibrations and all of them are IR and Raman active [25]. The calculated and observed vibrational wavenumbers using DFT/B3LYP/6-311++G(d,p) basis set, along with their relative intensities are given in **Table 2**. The total energy distribution (TED) was calculated using SQM program [26]. The

**Table 1** The optimized bond parameters of T<sub>2</sub>CNH.

Bond Parametres	B3LYP/6-311++G(d,p)	XRD <sup>a,b,c</sup>
Bond Lengths (Å)		
S1-C2	1.750	1.728 <sup>b</sup>
S1-C5	1.728	1.717 <sup>a</sup> , 1.707 <sup>b</sup>
C2-C3	1.377	1.375 <sup>a</sup> , 1.362 <sup>b</sup>
C2-C9	1.448	
C3-C4	1.418	1.431 <sup>a</sup> , 1.392 <sup>b</sup>
C3-H8	1.081	1.114 <sup>a</sup>
C4-C5	1.369	1.345 <sup>b</sup>
C9-H10	1.097	0.930 <sup>c</sup>
C9-N11	1.282	1.266 <sup>c</sup>
N11-N12	1.357	1.375 <sup>c</sup>
N12-H13	1.016	0.860 <sup>c</sup>
N12-C14	1.385	1.354 <sup>c</sup>
C14-O15	1.213	1.224 <sup>c</sup>
C16-C17	1.399	1.384 <sup>c</sup>
C16-C18	1.397	1.371 <sup>c</sup>
C17-N19	1.335	1.334 <sup>c</sup>
C17-H20	1.087	0.930 <sup>c</sup>
C18-C21	1.387	1.368 <sup>c</sup>
C18-H22	1.083	0.930 <sup>c</sup>
N19-C23	1.335	1.337 <sup>c</sup>
C21-C23	1.395	1.368 <sup>c</sup>
C23-H25	1.086	0.930 <sup>c</sup>
Bond Angles (°)		
C2-S1-C5	91.57	92.00 <sup>a</sup> , 91.81 <sup>b</sup>
S1-C2-C3	110.68	111.80 <sup>a</sup>
C2-C3-C4	113.02	112.20 <sup>a</sup> , 114.72 <sup>b</sup>
C2-C3-H8	122.16	129.20 <sup>a</sup>
C3-C4-C5	113.03	112.05 <sup>b</sup>
S1-C5-C4	111.68	112.13 <sup>b</sup>
N12-C14-C16	114.21	114.95 <sup>c</sup>
O15-C14-C16	122.13	121.48 <sup>c</sup>
C16-C17-N19	123.88	122.05 <sup>c</sup>
C16-C17-H20	120.91	120.03 <sup>c</sup>
N19-C17-H20	115.16	118.20 <sup>c</sup>
C16-C18-C21	118.94	118.91 <sup>c</sup>
C16-C18-H22	119.08	120.50 <sup>c</sup>
C21-C18-H22	121.96	120.30 <sup>c</sup>
C17-N19-C23	117.47	117.44 <sup>c</sup>
C18-C21-C23	118.58	118.58 <sup>c</sup>
C18-C21-H24	121.13	120.71 <sup>c</sup>
C23-C21-H24	120.27	120.70 <sup>c</sup>
N19-C23-C21	123.40	123.64 <sup>c</sup>
Dihedral Angles (°)		
S1-C2-C9-H10	-0.07	
S1-C2-C9-N11	-179.96	
C3-C2-C9-H10	179.93	
C3-C2-C9-N11	0.03	
C2-C3-C4-C5	0.02	
C2-C3-C4-H7	-179.98	
H8-C3-C4-C5	179.97	
H8-C3-C4-H7	-0.03	
C3-C4-C5-S1	-0.01	
C3-C4-C5-H6	-179.99	

H7-C4-C5-S1	179.99	
H7-C4-C5-H6	0.01	
C2-C9-N11-N12	179.45	
H10-C9-N11-N12	-0.43	
C9-N11-N12-H13	1.93	
C9-N11-N12-C14	175.56	
N11-N12-C14-O15	-2.82	
N11-N12-C14-C16	177.89	
H13-N12-C14-O15	170.80	
H13-N12-C14-C16	-8.47	
N12-C14-C16-C17	-28.41	
N12-C14-C16-C18	154.27	
O15-C14-C16-C17	152.29	
O15-C14-C16-C18	-25.01	
C14-C16-C17-N19	-178.88	
C14-C16-C17-H20	-0.97	
C18-C16-C17-N19	-1.57	

<sup>a</sup>Brathen O, Kveseth K, Nielsen KJ, Hagen K (1986) J Mol Struct 145: 45.  
<sup>b</sup>Geiger DK, Geiger HC, Williams L, Noll BC (2012) Acta Cryst E 68 : 0420.  
<sup>c</sup>Ramesh Babu N (2014) J Mol Struct 1072: 84-93.

combined vibrational spectra of T<sub>2</sub>CNH molecule are shown in **Figures 2 and 3**.

### N-H vibrations

The N-H stretching vibration appears in the region of 3300-3500 cm<sup>-1</sup> [27]. In accordance with the above literature the νN-H vibration has been observed at 3401 cm<sup>-1</sup> in FTIR spectrum, whereas the harmonic wavenumber assigned at 3365 cm<sup>-1</sup> (mode no: 1) and its TED value is 100% it should be noted here that, a small deviation between theoretical and experimental value is only due to intra-molecular charge transfer between amino and carbonyl group in hydrazone linkage. The harmonic wavenumbers (1508/ mode no: 14 and 488 cm<sup>-1</sup>/mode no: 53) of βN-H and γN-H modes were presented in **Table 2** are found to be in good agreement with literature [28] data 1476 and 535 cm<sup>-1</sup> as well as with the structurally related molecule. Mode no: 14 is in agreement with observed FT-Raman band at 1519 cm<sup>-1</sup> and these assignments also find support from TED values (22% and 61%).

### C-H vibrations

In aromatic compounds, the νCH, βCH and γCH vibrations are expected to appear in the ranges of 3100-3000 cm<sup>-1</sup>, 1400-1000 cm<sup>-1</sup> and 1000-750 cm<sup>-1</sup>, respectively [29,30]. In this study, the aromatic C-H stretching vibration is observed at 3059 cm<sup>-1</sup>/FT-IR, whereas the calculated wavenumbers are in the range 3076-3016 cm<sup>-1</sup> (mode nos. 5 and 9). The in-plane C-H bending vibrations are assigned at 1425, 1290 cm<sup>-1</sup> in FT-IR and 1429, 1300 & 1195 cm<sup>-1</sup> in FT-Raman spectra and their corresponding calculated wavenumbers are 1447, 1391, 1308, 1173 cm<sup>-1</sup> (mode nos: 16, 18, 21, 25). The harmonic wavenumbers occur in the region of 974-808 cm<sup>-1</sup> (mode nos: 34-36, 42) are assigned to C-H out-of-plane bending modes, in which mode no: 35 is in agreement with observed wavenumber values: 955 cm<sup>-1</sup> (FT-Raman) and 948 cm<sup>-1</sup> (FT-IR). These assignments are in line with literature values [14] and also find support from TED Values.

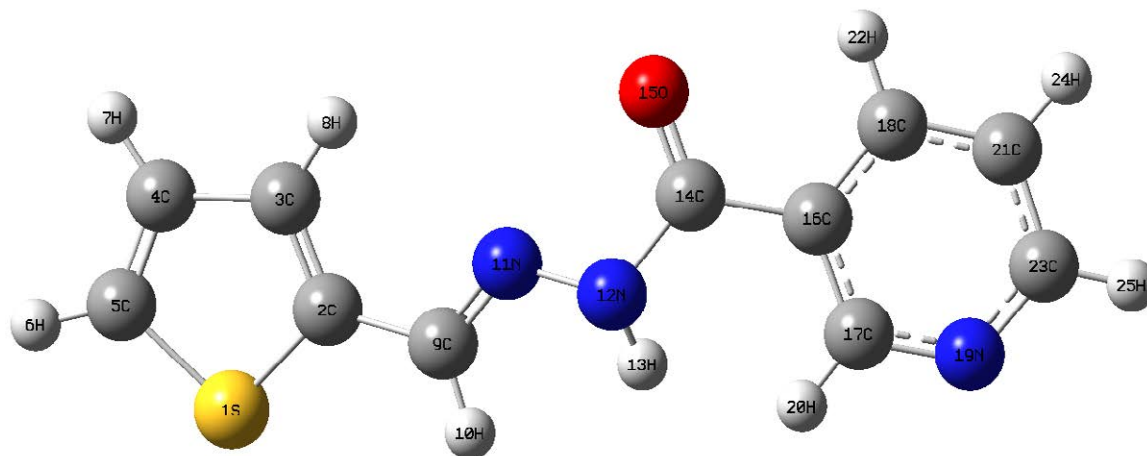


**Figure 1** The Optimized structure of (E)-N'-(thiophen-2-ylmethylene) nicotinohydrazide (T2CNH).

**Table 2** The experimental and calculated frequencies of T<sub>2</sub>CNH using B3LYP/6-311++G(d,p) level of basis set [harmonic frequencies (cm<sup>-1</sup>), IR, Raman intensities (Km/mol), reduced masses (amu) and force constants (mdynÅ<sup>-1</sup>)].

Mode No	Calculated Frequencies (cm <sup>-1</sup> )		Observed Frequencies (cm <sup>-1</sup> )		IR Intensity		Raman Intensity		Reduced Masses	Force Consts	Vibrational assignments ≥10% (TED) <sup>d</sup>
	Un Scaled	Scaled <sup>a</sup>	FT-IR	FT-Raman	Abs.	Rel. <sup>b</sup>	Abs.	Rel. <sup>c</sup>			
1	3503	3365	3401 w		7.42	2.06	134.41	1.67	1.08	7.78	vN <sub>12</sub> H <sub>13</sub> (100)
2	3247	3120	3171 w		1.23	0.34	101.27	1.26	1.10	6.82	vc <sub>5</sub> H <sub>6</sub> (94)
3	3223	3096			0.57	0.16	34.50	0.43	1.10	6.70	vc <sub>3</sub> H <sub>8</sub> (97)
4	3204	3078		3079 w	6.29	1.75	62.54	0.78	1.09	6.59	vc <sub>4</sub> H <sub>7</sub> (96)
5	3202	3076			7.00	1.94	72.48	0.90	1.10	6.62	vc <sub>18</sub> H <sub>22</sub> (99)
6	3187	3062	3059 w		9.14	2.54	84.20	1.05	1.09	6.53	vc <sub>21</sub> H <sub>24</sub> (95)
7	3156	3032			10.92	3.03	72.05	0.89	1.09	6.39	vc <sub>23</sub> H <sub>25</sub> (92)
8	3139	3016			29.24	8.12	29.47	0.37	1.09	6.32	vc <sub>17</sub> H <sub>20</sub> (99)
9	3019	2901			42.64	11.84	29.11	0.36	1.09	5.83	vc <sub>9</sub> H <sub>10</sub> (100)
10	1757	1688	1673 s	1670 w	360.16	100.00	392.18	4.87	11.08	20.16	vo <sub>15</sub> C <sub>14</sub> (85)
11	1656	1591	1592 s	1589 s	15.73	4.37	8057.31	100.00	7.23	11.68	vN <sub>11</sub> C <sub>9</sub> (75)+βH <sub>10</sub> C <sub>9</sub> N <sub>11</sub> (20)
12	1627	1563			32.79	9.10	1339.53	16.63	5.75	8.96	vc <sub>18</sub> C <sub>21</sub> (30)+vN <sub>19</sub> C <sub>23</sub> (30)+βC <sub>21</sub> C <sub>23</sub> N <sub>19</sub> (25)
13	1605	1542	1549 w		6.21	1.73	25.40	0.32	5.21	7.91	vc <sub>21</sub> C <sub>23</sub> (31)+vc <sub>16</sub> C <sub>18</sub> (27)+βC <sub>17</sub> N <sub>19</sub> C <sub>23</sub> (10)
14	1570	1508		1519 w	217.56	60.41	126.25	1.57	3.38	4.91	vc <sub>2</sub> C <sub>3</sub> (28)+βH <sub>13</sub> N <sub>12</sub> N <sub>11</sub> (22)+vc <sub>4</sub> C <sub>5</sub> (13)+vc <sub>2</sub> C <sub>9</sub> (11)
15	1551	1490			202.85	56.32	2133.94	26.48	2.19	3.10	vc <sub>2</sub> C <sub>3</sub> (14)+βH <sub>13</sub> N <sub>12</sub> N <sub>11</sub> (41)+vc <sub>4</sub> C <sub>5</sub> (12)
16	1506	1447	1425 m	1429 m	26.23	7.28	58.60	0.73	2.15	2.87	βH <sub>24</sub> C <sub>21</sub> C <sub>23</sub> (27)+βH <sub>20</sub> C <sub>17</sub> C <sub>16</sub> (25)
17	1459	1402			8.66	2.41	4817.87	59.80	4.83	6.07	vc <sub>2</sub> C <sub>3</sub> (13)+vc <sub>4</sub> C <sub>5</sub> (32)+βH <sub>7</sub> C <sub>4</sub> C <sub>5</sub> (14)+vc <sub>3</sub> C <sub>4</sub> (15)
18	1448	1391			26.37	7.32	62.23	0.77	2.18	2.69	βH <sub>25</sub> C <sub>23</sub> N <sub>19</sub> (43)+βC <sub>16</sub> C <sub>17</sub> N <sub>19</sub> (23)
19	1390	1335			52.04	14.45	1478.54	18.35	1.75	1.99	vc <sub>4</sub> C <sub>5</sub> (13)+βH <sub>10</sub> C <sub>9</sub> N <sub>11</sub> (38)+βH <sub>6</sub> C <sub>5</sub> C <sub>4</sub> (13)
20	1387	1333			16.34	4.54	60.17	0.75	2.08	2.36	βH <sub>10</sub> C <sub>9</sub> N <sub>11</sub> (25)+βH <sub>6</sub> C <sub>5</sub> C <sub>4</sub> (15)+vc <sub>3</sub> C <sub>4</sub> (18)
21	1362	1308	1290 s	1300 m	0.98	0.27	2.27	0.03	1.31	1.43	βH <sub>20</sub> C <sub>17</sub> C <sub>16</sub> (45)+βH <sub>22</sub> C <sub>18</sub> C <sub>21</sub> (23)
22	1291	1240		1241 w	19.71	5.47	141.74	1.76	7.28	7.15	vN <sub>19</sub> C <sub>23</sub> (43)+vc <sub>16</sub> C <sub>18</sub> (27)
23	1268	1219	1218 m	1225 w	94.23	26.16	45.69	0.57	1.54	1.46	βH <sub>7</sub> C <sub>4</sub> C <sub>5</sub> (23)+βH <sub>8</sub> C <sub>3</sub> C <sub>4</sub> (29)+βH <sub>6</sub> C <sub>5</sub> C <sub>4</sub> (13)
24	1265	1215			221.71	61.56	2432.18	30.19	2.39	2.25	vc <sub>14</sub> C <sub>16</sub> (22)
25	1221	1173		1195 w	39.47	10.96	610.76	7.58	1.60	1.40	vc <sub>18</sub> C <sub>21</sub> (11)+βH <sub>24</sub> C <sub>21</sub> C <sub>23</sub> (17)+βH <sub>25</sub> C <sub>23</sub> N <sub>19</sub> (30)
26	1195	1148	1145 m	1149 w	87.67	24.34	456.90	5.67	3.39	2.85	vN <sub>11</sub> N <sub>12</sub> (60)
27	1142	1097		1096 w	146.68	40.73	527.62	6.55	2.70	2.07	vc <sub>2</sub> C <sub>9</sub> (10)+vN <sub>12</sub> C <sub>14</sub> (40)
28	1134	1090			69.91	19.41	242.18	3.01	1.45	1.10	βH <sub>24</sub> C <sub>21</sub> C <sub>23</sub> (20)+βC <sub>16</sub> C <sub>17</sub> N <sub>19</sub> (12)+βH <sub>22</sub> C <sub>18</sub> C <sub>21</sub> (36)
29	1102	1059			7.47	2.07	295.96	3.67	1.26	0.90	vc <sub>4</sub> C <sub>5</sub> (15)+βH <sub>7</sub> C <sub>4</sub> C <sub>5</sub> (22)+βH <sub>6</sub> C <sub>5</sub> C <sub>4</sub> (47)
30	1086	1044			5.12	1.42	134.46	1.67	3.17	2.21	vN <sub>11</sub> N <sub>12</sub> (24)+vN <sub>12</sub> C <sub>14</sub> (16)
31	1058	1017	1031 w	1030 w	1.76	0.49	393.20	4.88	3.19	2.11	βC <sub>16</sub> C <sub>18</sub> C <sub>21</sub> (45)

32	1056	1015			7.59	2.11	414.19	5.14	1.76	1.15	$\beta\text{H}_7\text{C}_4\text{C}_5(14)+\beta\text{H}_8\text{C}_3\text{C}_4(27)+\nu\text{C}_3\text{C}_4(35)$
33	1039	999			11.95	3.32	318.45	3.95	4.30	2.73	$\beta\text{C}_{17}\text{N}_{19}\text{C}_{23}(32)+\beta\text{C}_{21}\text{C}_2\text{N}_{19}(15)+\beta\text{C}_{18}\text{C}_{21}\text{C}_{23}(25)$
34	1014	974			2.23	0.62	6.67	0.08	1.38	0.83	$\tau\text{H}_{22}\text{C}_{18}\text{C}_{21}\text{H}_{24}(75)+\text{FC}_{23}\text{C}_{21}\text{N}_{19}\text{H}_{25}(18)$
35	987	949	948 w	955 w	0.58	0.16	8.33	0.10	1.43	0.82	$\text{FC}_{23}\text{C}_{21}\text{N}_{19}\text{H}_{25}(50)+\text{FC}_{17}\text{C}_{16}\text{N}_{19}\text{H}_{20}(12)+\text{FC}_{18}\text{C}_{16}\text{C}_2\text{H}_{22}(30)$
36	947	910			1.90	0.53	6.99	0.09	1.39	0.73	$\text{FC}_{17}\text{C}_{16}\text{N}_{19}\text{H}_{20}(71)$
37	945	908		904 w	9.84	2.73	50.68	0.63	1.50	0.79	$\text{FH}_{10}\text{C}_9\text{N}_{11}\text{H}_{12}(80)$
38	928	891	897 w		0.39	0.11	6.15	0.08	1.38	0.70	$\tau\text{H}_6\text{C}_5\text{C}_4\text{H}_7(46)+\text{FC}_3\text{C}_2\text{C}_4\text{H}_8(32)$
39	921	885			38.10	10.58	86.38	1.07	7.12	3.56	$\beta\text{N}_{12}\text{C}_{14}\text{O}_{15}(20)+\beta\text{C}_{14}\text{N}_{12}\text{N}_{11}(25)$
40	861	827	846 w		31.22	8.67	114.39	1.42	4.31	1.88	$\beta\text{C}_4\text{C}_5\text{S}_1(80)$
41	851	817			8.44	2.34	1.04	0.01	1.29	0.55	$\tau\text{H}_6\text{C}_5\text{C}_4\text{H}_7(36)+\text{FC}_3\text{C}_2\text{C}_4\text{H}_8(55)$
42	841	808			13.98	3.88	48.48	0.60	1.97	0.82	$\tau\text{H}_{22}\text{C}_{18}\text{C}_{21}\text{H}_{24}(17)+\text{FC}_{23}\text{C}_{21}\text{N}_{19}\text{H}_{25}(12)+\text{FC}_{18}\text{C}_{16}\text{C}_{21}\text{H}_{22}(32)+\text{FO}_{15}\text{C}_{16}\text{N}_{12}\text{C}_{14}(12)$
43	823	791			25.89	7.19	107.27	1.33	4.43	1.77	$\nu\text{C}_2\text{C}_3(10)+\beta\text{C}_2\text{C}_9\text{N}_{11}(20)+\nu\text{S}_1\text{C}_2(17)$
44	747	718			3.22	0.89	221.87	2.75	7.15	2.35	$\beta\text{C}_2\text{C}_3\text{C}_4(57)+\nu\text{S}_1\text{C}_2(23)$
45	739	710	700 w		31.92	8.86	64.22	0.80	2.76	0.89	$\text{FC}_{18}\text{C}_{16}\text{C}_2\text{H}_{22}(25)+\text{FO}_{15}\text{C}_{16}\text{N}_{12}\text{C}_{14}(50)$
46	724	695			21.84	6.06	20.02	0.25	4.31	1.33	$\beta\text{C}_{21}\text{C}_{23}\text{N}_{19}(17)+\tau\text{C}_{16}\text{C}_{17}\text{C}_{23}\text{N}_{19}(16)+\tau\text{C}_{16}\text{C}_{18}\text{C}_{23}\text{C}_{21}(16)+\tau\text{C}_{18}\text{C}_{21}\text{N}_{19}\text{C}_{23}(10)$
47	718	690			16.37	4.54	7.30	0.09	3.96	1.20	$\tau\text{C}_{16}\text{C}_{17}\text{C}_{23}\text{N}_{19}(27)+\tau\text{C}_{16}\text{C}_{18}\text{C}_{23}\text{C}_{21}(22)+\tau\text{C}_{18}\text{C}_{21}\text{N}_{19}\text{C}_{23}(16)$
48	706	679		652 w	75.61	20.99	10.36	0.13	1.17	0.34	$\tau\text{H}_6\text{C}_5\text{C}_4\text{H}_7(13)+\tau\text{H}_6\text{C}_5\text{S}_1\text{C}_2(81)$
49	633	608	607 s		4.00	1.11	49.48	0.61	7.72	1.82	$\beta\text{C}_{16}\text{C}_{17}\text{N}_{19}(15)+\beta\text{C}_{17}\text{N}_{19}\text{C}_{23}(15)+\beta\text{C}_{18}\text{C}_{21}\text{C}_{23}(41)$
50	610	586			2.58	0.72	360.42	4.47	9.05	1.98	$\beta\text{C}_2\text{S}_1\text{C}_5(63)$
51	586	563			1.22	0.34	16.70	0.21	3.25	0.66	$\tau\text{C}_3\text{C}_2\text{C}_4\text{H}_5(79)$
52	528	507	503 m		15.76	4.38	167.78	2.08	3.01	0.49	$\beta\text{C}_{16}\text{C}_{14}\text{N}_{12}(22)+\tau\text{H}_{13}\text{N}_{12}\text{C}_{14}\text{C}_{16}(22)+\text{FC}_{14}\text{C}_{16}\text{C}_1\text{C}_8(10)$
53	508	488			44.93	12.47	72.78	0.90	1.60	0.24	$\tau\text{H}_{13}\text{N}_{12}\text{C}_{14}\text{C}_{16}(61)$
54	492	472			0.31	0.09	8.91	0.11	4.01	0.57	$\tau\text{C}_2\text{S}_1\text{C}_4\text{C}_5(65)$
55	451	433			0.46	0.13	24.54	0.30	7.97	0.95	$\beta\text{C}_2\text{C}_9\text{N}_{11}(14)+\nu\text{S}_1\text{C}_2(12)+\beta\text{C}_{17}\text{C}_{16}\text{C}_{18}(10)+\beta\text{C}_9\text{C}_2\text{S}_1(12)+\beta\text{C}_{14}\text{N}_{12}\text{N}_{11}(11)$
56	419	402			7.99	2.22	9.91	0.12	4.68	0.48	$\tau\text{C}_{16}\text{C}_{17}\text{C}_{23}\text{N}_{19}(15)+\tau\text{C}_{16}\text{C}_{18}\text{C}_{23}\text{C}_{21}(31)$
57	396	381			4.89	1.36	11.97	0.15	3.36	0.31	$\tau\text{C}_{16}\text{C}_{18}\text{C}_{23}\text{C}_{21}(16)+\tau\text{C}_{18}\text{C}_{21}\text{N}_{19}\text{C}_{23}(34)+\text{FC}_{14}\text{C}_{16}\text{C}_1\text{C}_8(10)$
58	379	364			1.32	0.37	1.86	0.02	8.03	0.68	$\nu\text{C}_{14}\text{C}_{16}(17)+\beta\text{N}_{12}\text{C}_{14}\text{O}_{15}(22)+\beta\text{C}_{17}\text{C}_{16}\text{C}_{18}(20)$
59	340	326			1.88	0.52	29.62	0.37	5.99	0.41	$\tau\text{C}_2\text{S}_1\text{C}_4\text{C}_5(18)+\tau\text{C}_2\text{C}_9\text{N}_{11}\text{N}_{12}(34)$
60	264	253			13.84	3.84	34.50	0.43	4.73	0.19	$\beta\text{C}_{14}\text{C}_{16}\text{C}_{18}(36)$
61	226	217		224 w	11.59	3.22	71.81	0.89	3.69	0.11	$\tau\text{C}_2\text{S}_1\text{C}_2\text{C}_9(11)+\text{FC}_{16}\text{C}_{14}\text{N}_{12}\text{N}_{11}(20)+\tau\text{C}_3\text{C}_2\text{C}_9\text{N}_{11}(16)$
62	213	205		191 w	1.15	0.32	136.24	1.69	10.18	0.27	$\beta\text{C}_9\text{C}_2\text{S}_1(30)+\beta\text{C}_{14}\text{N}_{12}\text{N}_{11}(22)$
63	170	163			11.98	3.33	135.90	1.69	4.69	0.08	$\tau\text{C}_9\text{N}_{11}\text{N}_{12}\text{C}_{14}(20)+\text{FC}_{14}\text{C}_{16}\text{C}_{18}\text{C}_{17}(14)+\tau\text{C}_3\text{C}_2\text{C}_9\text{N}_{11}(13)$
64	130	125			1.52	0.42	83.59	1.04	5.74	0.06	$\tau\text{C}_9\text{N}_{11}\text{N}_{12}\text{C}_{14}(25)+\tau\text{C}_5\text{S}_1\text{C}_2\text{C}_9(37)+\text{FC}_{14}\text{C}_{16}\text{C}_{18}\text{C}_{17}(10)$
65	120	115			6.55	1.82	60.10	0.75	5.71	0.05	$\beta\text{C}_2\text{C}_9\text{N}_{11}(18)+\beta\text{C}_{16}\text{C}_{14}\text{N}_{12}(18)+\beta\text{C}_9\text{C}_2\text{S}_1(17)+\text{FC}_{14}\text{C}_{16}\text{C}_{18}\text{C}_{17}(14)$
66	64	61		80 m	5.89	1.63	381.03	4.73	5.90	0.01	$\tau\text{C}_5\text{S}_1\text{C}_2\text{C}_9(12)+\tau\text{C}_{18}\text{C}_{16}\text{C}_{14}\text{N}_{12}(45)+\tau\text{C}_3\text{C}_2\text{C}_9\text{N}_{11}(15)$
67	46	45			0.73	0.20	161.56	2.01	6.68	0.01	$\beta\text{C}_2\text{C}_9\text{N}_{11}(16)+\beta\text{C}_{16}\text{C}_{14}\text{N}_{12}(14)+\beta\text{C}_9\text{N}_{11}\text{N}_{12}(20)+\beta\text{C}_{14}\text{N}_{12}\text{N}_{11}(22)$
68	32	31			1.86	0.52	329.50	4.09	5.69	0.00	$\tau\text{C}_2\text{C}_9\text{N}_{11}\text{N}_{12}(18)+\tau\text{C}_{18}\text{C}_{16}\text{C}_{14}\text{N}_{12}(15)+\tau\text{C}_{16}\text{C}_{14}\text{N}_{12}\text{N}_{11}(49)$
69	27	26			0.47	0.13	967.33	12.01	5.46	0.00	$\tau\text{C}_9\text{N}_{11}\text{N}_{12}\text{C}_{14}(18)+\tau\text{C}_{18}\text{C}_{16}\text{C}_{14}\text{N}_{12}(25)+\tau\text{C}_3\text{C}_2\text{C}_9\text{N}_{11}(18)$

v: Stretching,  $\beta$ : in-plane-bending,  $\Gamma$ : out-of-plane bending,  $\tau$ - Torsion, vw: very week, w:week, m:medium, s:strong, vs: very strong.

<sup>a</sup>Scaling factor: 0.9608.

<sup>b</sup>Relative IR absorption intensities normalized with highest peak absorption equal to 100.

<sup>c</sup>Relative Raman intensities calculated by Equation (1) and normalized to 100.

<sup>d</sup>Total energy distribution calculated at B3LYP/6-311++G(d,p) level.



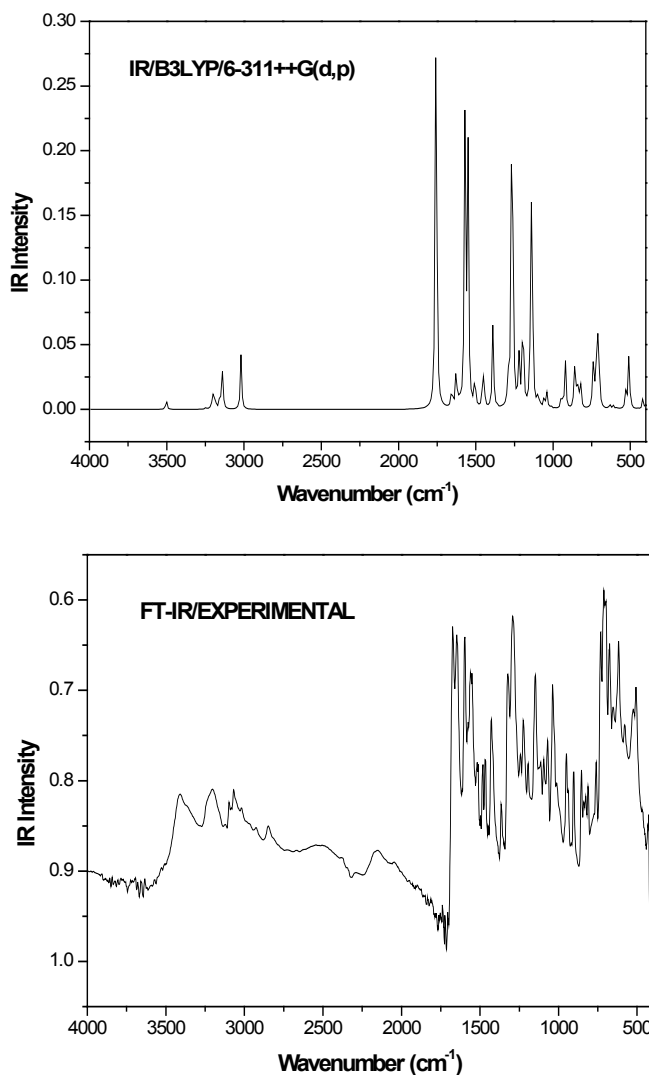


**Figure 2** The Theoretical and Experimental FT-IR spectra of  $T_2CNH$ .

The  $\nu_{CH}$  modes are expected to appear in the range of 3100-3000  $cm^{-1}$  with multiple weak bands and the bands are not affected appreciably by the nature of the substituent's [31,32]. The  $\nu_{C-H}$  vibration of the thiophen ring is observed at 3171  $cm^{-1}$  in FT-IR and 3079  $cm^{-1}$  in FT-Raman spectra in accordance with the literature [20-22]. The harmonic values corresponding to  $\nu_{C-H}$  are calculated in the range 3120-3078  $cm^{-1}$  (mode nos: 2-4) with TED values >96%. This indicates that these are highly pure stretching modes. The  $\beta_{C-H}$  vibrations appear by sharp but weak to medium bands in the range 1100-1500  $cm^{-1}$  and the bands are not sensitive to the nature of substituents. The  $\gamma_{C-H}$  deformation modes are expected to appear in the range 800-1000  $cm^{-1}$  [32]. The IR active  $\beta_{C-H}/\gamma_{C-H}$  vibrations of  $T_2CNH$  molecule are observed at 1218/897  $cm^{-1}$ , respectively. The harmonic wavenumbers of these bands are 1219, 1059, 1015 and 891, 817  $cm^{-1}$  in good agreement with literature values [20-22].

The harmonic frequencies for  $\nu_{C-H}$ ,  $\beta_{C-H}$  and  $\gamma_{C-H}$  modes in hydrozone linkage were assigned at 2919, 1315 and 910  $cm^{-1}$ , respectively and these assignments are in line with assignments  $\nu_{C-H}$ : 2901,  $\beta_{C-H}$ : 1335,  $\gamma_{C-H}$ : 908  $cm^{-1}$  (mode nos: 9, 19, 37) are

made in the present study. These vibrational assignments are further supported by literature [28] and TED output.

### C=C, C-C vibrations

In the pyridine ring, the  $\nu(C-C)$  stretching vibrations are usually occur in the ranges of 1590-1640, 1560-1580 and 1470-1510  $cm^{-1}$  [33]. The computed wavenumber for  $\nu(C-C)$  modes are lies at 1563, 1542, 1240 and 1173  $cm^{-1}$  (mode nos: 12, 13, 22 and 25) with TED values. In the present study it has been established well and the FTIR band at 1549  $cm^{-1}$  and FT-Raman bands at 1241, 1195  $cm^{-1}$  are designated as  $\nu_{C-C}$  vibrations. These assignments are find support from the literature [34] and also from TED values.

The bands arising from  $\beta_{CCC}$  and  $\gamma_{CCC}$  of pyridine moiety are ascribed to bands observed at 1031, 607 and 503  $cm^{-1}$  respectively in FTIR spectrum. These vibrational assignments find support from harmonic bands: 1017, 999, 608 and 507, 381, 163  $cm^{-1}$  (mode nos: 31, 33, 49 and 52, 57, 63) in addition to literature values [35].

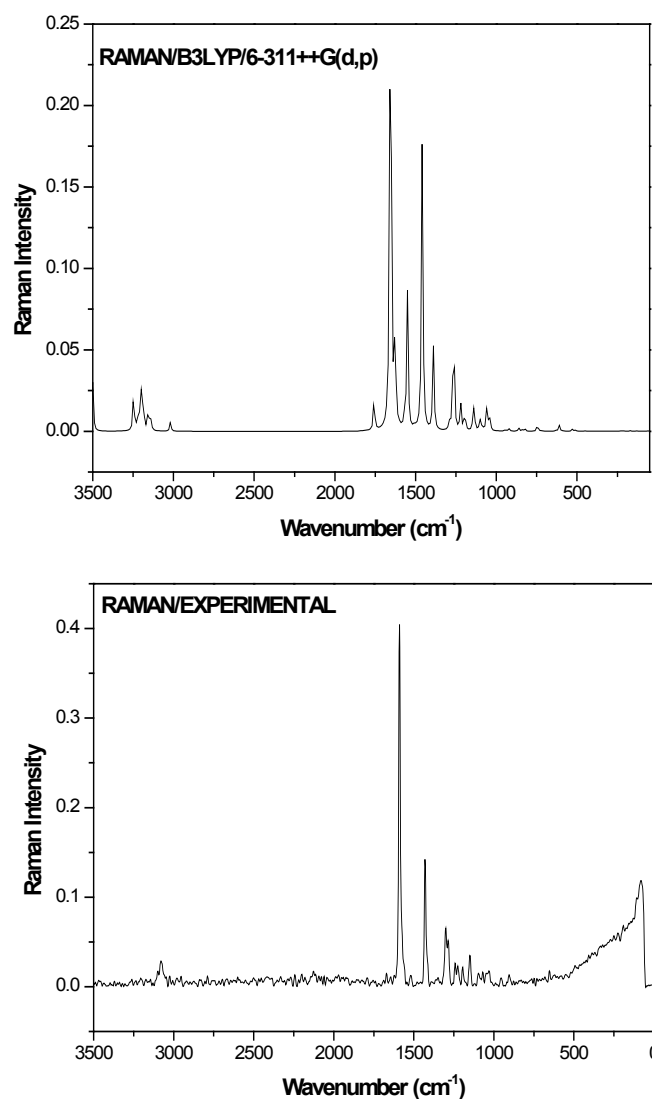
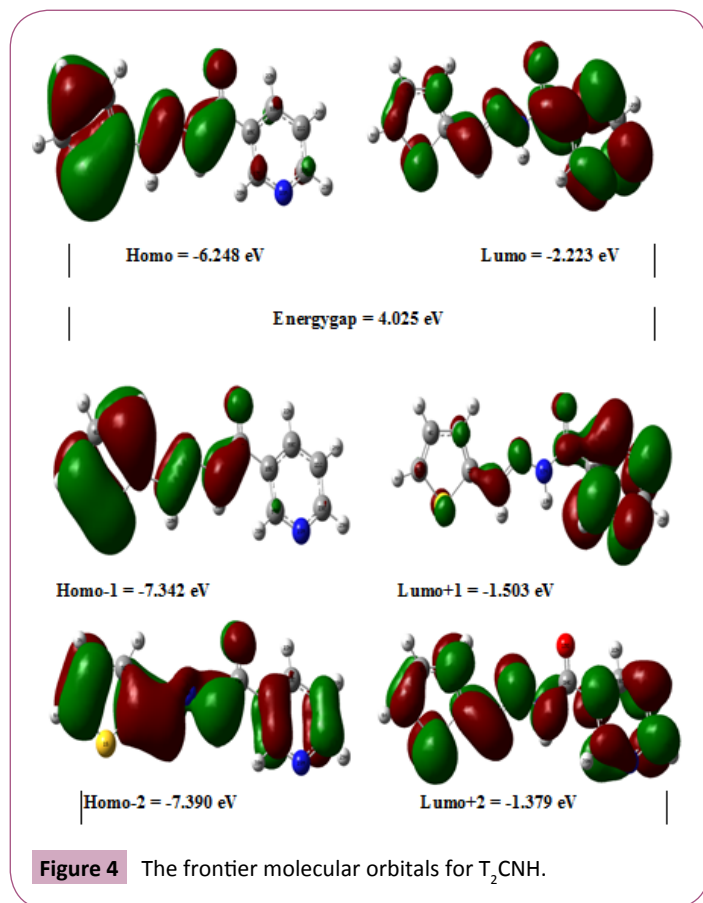


**Figure 3** The Theoretical and Experimental FT-Raman spectra of  $T_2CNH$ .



The ring carbon-carbon stretching vibrations in thiophen ring are reported in the ranges of 1329-1431, 1420-1501 and 1419-1519  $\text{cm}^{-1}$ , respectively [20-22]. For the same mode the computed wavenumbers are: 1508 (C=C), 1490 (C=C) and 1402  $\text{cm}^{-1}$  (C-C). These assignments are having considerable TED values  $\geq 15\%$  and its corresponding mode no: 14 is further supported by observed Raman band 1519  $\text{cm}^{-1}$ . The  $\beta\text{CCC}$  mode of thiophene moiety is ascribed to mode no: 44 (718  $\text{cm}^{-1}$ ), this supported by TED value (57%) also. The mode nos: 27 and 24 are attributed to  $\nu\text{C}_2\text{-C}_9$  and  $\nu\text{C}_{14}\text{-C}_{16}$  mode and are in agreement with literature [28].

### C=N, C-N vibrations

The identifications of C=N and C-N vibrations is a difficult task, since the mixing of vibrations is possible in this region [36]. However, with the help of Gauss View (3.0) software and TED results, those vibrations are described and assigned in this study. The C=N and C-N stretching vibrations appear in the ranges of 1670-1600  $\text{cm}^{-1}$  and 1382-1266  $\text{cm}^{-1}$  respectively [36]. In hydrozone linkage, the  $\nu\text{C}_9\text{=N}_{11}$  and  $\nu\text{C}_{14}\text{-N}_{12}$  stretching vibrations are assigned respectively at 1592  $\text{cm}^{-1}$  (FTIR) /1589  $\text{cm}^{-1}$  (FT-Raman) and at 1096  $\text{cm}^{-1}$  (FT-Raman). The TED results show that these vibrations are mixed with  $\beta\text{HCN}$  and  $\nu\text{C-C}$  modes and their corresponding harmonic frequencies are 1591 (mode no: 11) and 1097  $\text{cm}^{-1}$  (mode no: 27) well correlated with experimental observations. These vibrational assignments are also supported by literature [28] in addition to TED output (75% and 40%).

In pyridine ring, the harmonic/observed bands at 1563 (mode no: 12), 1240 (mode no: 22)/1241  $\text{cm}^{-1}$  in FT-Raman spectrum can be assigned to C-N stretching vibration and TED also predict that these vibrations are mixed with  $\nu\text{C-C}$  modes. These assignments are in good agreement with our earlier study [28] and also find support from TED values (30%, 43%). The  $\beta\text{C}_{21}\text{-C}_{23}\text{-N}_{19}$ ,  $\beta\text{C}_{16}\text{-C}_{17}\text{-N}_{19}$ ,  $\beta\text{C}_{17}\text{-N}_{19}\text{-C}_{23}$  and  $\beta\text{C}_2\text{-C}_9\text{=N}_{11}$ ,  $\beta\text{C}_{16}\text{-C}_{14}\text{-N}_{12}$  deformations belong to pyridine and hydrozone moieties, respectively assigned to 1563, 1391, 999 and 791, 507  $\text{cm}^{-1}$  (mode nos: 12, 18, 33 and 43, 52). Similarly the  $\tau\text{C}_{16}\text{C}_{17}\text{C}_{23}\text{N}_{19}$ ,  $\tau\text{C}_{18}\text{C}_{21}\text{N}_{19}\text{C}_{23}$ ,  $\tau\text{C}_3\text{C}_2\text{C}_9\text{N}_{11}$ ,  $\Gamma\text{C}_{16}\text{C}_{14}\text{N}_{12}\text{N}_{11}$  modes are assigned to wavenumbers: 690, 381, 217, 217  $\text{cm}^{-1}$  (mode nos: 47, 57, 61, 61).

### N-N vibrations

The  $\nu\text{N-N}$  stretching was observed at 1145  $\text{cm}^{-1}$  in FTIR is undoubtedly assigned to  $\nu\text{N}_{11}\text{-N}_{12}$  vibration and the value of this band is calculated at 1148  $\text{cm}^{-1}$  (mode no: 26) with a TED of (60%) [28]. This assignment is well correlated with observed FT-Raman band 1149  $\text{cm}^{-1}$ . The in-plane bending vibrations of  $\text{C}_2\text{-C}_9\text{=N}_{11}$ ,  $\text{C}_9\text{=N}_{11}\text{-N}_{12}$  &  $\text{C}_{14}\text{-N}_{12}\text{-N}_{11}$  are assigned to wavenumbers: 791, 45 & 885, having considerable TED values ( $\geq 20\%$ ). The wavenumbers 163, 326  $\text{cm}^{-1}$  (mode nos: 63, 59) are assigned to  $\tau\text{C}_9\text{=N}_{11}\text{-N}_{12}\text{-C}_{14}$ ,  $\tau\text{C}_2\text{-C}_9\text{=N}_{11}\text{-N}_{12}$  modes.

### C-S vibrations

In T2CNH the scaled wavenumbers 791 and 718  $\text{cm}^{-1}$  (mode nos: 43 and 44) are assigned to  $\nu\text{C-S}$  modes of thiophen ring moiety. This assignment is in agreement with the assignments proposed by various authors [20,21]. This mode is well known to mix with neighboring modes ( $\nu\text{CC}$ ,  $\beta\text{CCN}$ /mode no: 43 and  $\beta\text{CCC}$ /mode no: 44) as reported in the literature [37]. The harmonic frequencies of  $\beta\text{CSC}$  and  $\Gamma\text{CSC}$  vibrations are ascribed to wavenumbers: 586  $\text{cm}^{-1}$  (mode no: 50) and 125  $\text{cm}^{-1}$  (mode no: 64) with 62% and 37% of TED values, respectively. Further the wavenumbers 827  $\text{cm}^{-1}$  (mode no: 40) and 205  $\text{cm}^{-1}$  (mode no: 62) are assigned to  $\beta\text{C}_4\text{C}_5\text{S}_1$  and  $\beta\text{C}_9\text{C}_2\text{S}_1$  modes, respectively, which are in line with the observed bands (846  $\text{cm}^{-1}$ : FTIR and 191  $\text{cm}^{-1}$ : FT-Raman) in addition to support the TED values [80% and 30%].

### C=O vibrations

The C=O is formed by  $\text{P}\pi\text{-P}\pi$  bonding between carbon and oxygen atoms. Carbonyl (C=O) group stretching vibration is expected to appear in the region of 1680-1715  $\text{cm}^{-1}$  [38]. In this study, the carbonyl group stretching vibration appear at 1670  $\text{cm}^{-1}$  as strong band in FT-IR and at 1673  $\text{cm}^{-1}$  as weak band in FT-Raman spectra. The values of  $\nu\text{C=O}$  band is calculated at 1688  $\text{cm}^{-1}$  (mode no: 10) with a TED of 85%. The  $\beta\text{C=O}$  and  $\Gamma\text{C=O}$  vibrations are assigned respectively to mode nos: 39 and 45, in which the predicted wavenumber related to  $\Gamma\text{C=O}$  mode is found to be in moderate agreement with the observed FTIR band at 700  $\text{cm}^{-1}$ .

### NLO Property

Analysis of organic compounds having conjugated  $\pi$ -electron systems and large hyperpolarizability using IR and Raman spectroscopy has evolved as a subject of scientific research. The application of the title molecule in the field of non-linear optics demands the investigation of its structural and bonding features

contributing to the hyperpolarizability enhancement by analyzing the vibrational modes using IR and Raman spectroscopy. The DFT/B3LYP/6-311++G(d,p) basis set has been used for the prediction of first hyperpolarizability.

The calculated first hyperpolarizability and the total molecular dipole moment of T2CNH is  $1.5861 \times 10^{-30}$  esu, 0.9906 Debye, respectively obtained by B3LYP/6-311++G(d,p) level of theory. The total dipole moment of the title molecule is moderately equal and  $\beta_0$  value of T2CNH is 4 times greater than that of urea, hence the molecule T2CNH has considerable non-linear optical (NLO) activity and the hyperpolarizabilities of T2CNH are given in **Table 3**.

## NBO Analysis

This method gives information about the intra- and inter-molecular interactions among bonds. Furthermore, it provides a convenient basis for investigating the interactions in both filled and virtual orbital spaces along with charge transfer and conjugative interactions in molecular system [39]. The natural bonding orbital (NBO) analysis was performed for T2CNH using B3LYP/6-311++G(d,p) basis set in order to elucidate the intra-molecular, hybridization and delocalization of ED within T2CNH. The strong intra-molecular hyperconjugative interaction of the  $\sigma$  and  $\pi$  electrons of C-C to the anti C-C bond of the pyridine ring leads to stabilization of some part of the pyridine ring. The NBO analysis has been carried out by B3LYP/6-311++G(d,p) basis set and the E(2) values and types of the transition are shown in **Table 4**.

**Table 3** The NLO measurements of T<sub>2</sub>CNH.

Parameters	B3LYP/6-311++G(d,p)
<b>Dipole moment ( <math>\mu</math> )</b>	<b>Debye</b>
$\mu_x$	0.3145
$\mu_y$	-0.7701
$\mu_z$	0.5380
$\mu$	0.9906Debye
<b>Polarizability ( <math>\alpha_0</math> )</b>	<b><math>\times 10^{-30}</math>esu</b>
$\alpha_{xx}$	330.88
$\alpha_{xy}$	-3.11
$\alpha_{yy}$	168.52
$\alpha_{xz}$	-4.63
$\alpha_{yz}$	-0.11
$\alpha_{zz}$	97.39
$\alpha_0$	0.5318 $\times 10^{-30}$ esu
<b>Hyperpolarizability ( <math>\beta_0</math> )</b>	<b><math>\times 10^{-30}</math>esu</b>
$\beta_{xxx}$	-1853.85
$\beta_{xxy}$	229.60
$\beta_{xyy}$	-33.45
$\beta_{yyy}$	-129.96
$\beta_{xxz}$	40.31
$\beta_{xyz}$	21.11
$\beta_{yyz}$	2.92
$\beta_{xzz}$	54.46
$\beta_{yzz}$	-29.90
$\beta_{zzz}$	-38.55
$\beta_0$	1.5861 $\times 10^{-30}$ esu

Standard value for urea ( $\mu=1.3732$  Debye,  $\beta_0=0.3728 \times 10^{-30}$  esu): esu-electrostatic unit

The larger E(2) value shows the intensive interaction between electron donors and electron acceptors. The strong intra-molecular hyper conjugative interactions of the  $\sigma$  and  $\pi$  electrons of the C=C, C=N to the anti C=C, C=N bond of the ring as well as C=O group leads to stabilization of some part of the ring system in T<sub>2</sub>CNH. In the present study, the  $\pi$ -character of the bond plays an important role on comparing with  $\sigma$  bond character. The hyper conjugative interactions  $\pi(C_2-C_3) \rightarrow \pi^*(C_9-N_{11})$ ,  $\pi(C_4-C_5) \rightarrow \pi^*(C_2-C_3)$ ,  $\pi(C_{16}-C_{17}) \rightarrow \pi^*(C_{18}-C_{21})$ ,  $\pi(C_{18}-C_{21}) \rightarrow \pi^*(N_{19}-C_{23})$ ,  $\pi(N_{19}-C_{23}) \rightarrow \pi^*(C_{16}-C_{17})$  and  $\pi(C_{14}-O_{15}) \rightarrow \pi^*(C_{16}-C_{17})$  transfer stabilization energy: 76.65, 66.02, 89.54, 122.13, 112.97 and 15.10 KJ/mol to the molecular system. The lone pair of sulphur, nitrogen and oxygen atoms play great role in T<sub>2</sub>CNH molecule. The S<sub>1</sub>, N<sub>12</sub> & O<sub>15</sub> atoms transfer maximum energy 91.55, 190.41 and 118.20 KJ/mol to (C<sub>4</sub>-C<sub>5</sub>), (C<sub>14</sub>-O<sub>15</sub>) & (N<sub>12</sub>-C<sub>14</sub>) bonds, respectively. The maximum hyperconjugative E(2) energy of heteroatoms during the inter-molecular interaction leads the molecule towards medicinal and biological applications [28]. The bond  $\sigma(C_3-H_8)$  transfer more energy (23.39 KJ/mol) to  $\sigma^*(S_1-C_2)$  bond on comparing with energy transfer (18.95 KJ/mol) from  $\sigma(C_4-H_7)$  to  $\sigma^*(S_1-C_5)$ . Hence the  $\nu(S_1-C_2)$  mode observe at higher frequency 791 cm<sup>-1</sup> (mode no: 43) than the  $\nu(S_1-C_5)$  mode (718 cm<sup>-1</sup>/mode no: 44).

## HOMO-LUMO Analysis

The highest occupied molecular orbital (HOMO) and lowest unoccupied molecular orbital (LUMO) analysis is very important parameters for quantum chemistry. The energy values of HOMO ( $\pi$ -donor) and LUMO ( $\pi$ -acceptor) and its energy gap which reflects the chemical activity of the molecule. The HOMO and LUMO energy was calculated by B3LYP/6-311++G(d,p) level of theory. The frontier molecular orbitals (FMOs) of T2CNH are listed in **Table 5**. The atomic compositions of FMOs are shown in **Figure 4**. The HOMO is located over the thiophene and hydrozone moieties. The LUMO is located over pyridine ring. The LUMO transition implies that an ED transfer to pyridine ring via hydrazone linkage. The HOMO and LUMO energies are predicted as -6.248 eV and -2.223 eV, respectively. The calculated HOMO-LUMO energy gap is 4.025 eV, which explains the eventual charge transfer taking place within the present molecule. The physico-chemical properties are also listed in **Table 6**.

## UV-Vis Spectral Analysis

The UV-Visible absorption spectrum of T2CNH was recorded in the range of 250-350 nm is shown in **Figure 5**. All the structures allow strong  $\pi$ - $\pi^*$  (or)  $\sigma$ - $\sigma^*$  transition in the UV-Vis region with high extinction coefficients. On the basis of fully optimized ground state structure at TD-DFT/B3LYP/6-311++G(d,p) calculation has been used to determine the low-lying excited states of T<sub>2</sub>CNH. The calculated results involving the vertical excitation energies, oscillator strength (f) and wavelength are carried out and compared with measured experimental wavelength. Typically, according to Franck-Condon principle, the maximum absorption peaks ( $\lambda_{max}$ ) in a UV-Vis spectrum corresponds to vertical excitation. It is evident from the **Table 7** that the calculated absorption maxima values have been found to be 332, 301 and



**Table 4** The second order perturbation theory analysis of Fock Matrix in NBO basis for T2CNH.

Type	Donor NBO (i)	ED/e	Acceptor NBO (j)	ED/e	E <sup>(2)</sup> kJ/mol	E(j)-E(i) a.u.	F(i,j) a.u.
$\pi$ - $\pi^*$	BD (2) C2 - C3	1.795	BD*(2) C4 - C5	0.309	69.58	0.28	0.06
			BD*(2) C9 - N11	0.209	76.65	0.28	0.06
$\sigma$ - $\sigma^*$	BD (1) C3 - H8	1.972	BD*(1) S1 - C2	0.028	23.39	0.73	0.06
			BD*(1) C2 - C3	0.021	7.57	1.12	0.04
			BD*(1) C4 - C5	0.014	8.08	1.11	0.04
$\pi$ - $\pi^*$	BD (2) C4 - C5	1.846	BD*(2) C2 - C3	0.351	66.02	0.30	0.06
$\sigma$ - $\sigma^*$	BD (1) C4 - H7	1.976	BD*(1) S1 - C5	0.017	18.95	0.75	0.05
			BD*(1) C2 - C3	0.021	8.03	1.12	0.04
			BD*(1) C4 - C5	0.014	5.73	1.12	0.04
$\pi$ - $\pi^*$	BD (2) C14 - O15	1.980	BD*(2) C16 - C17	0.335	15.10	0.40	0.04
$\pi$ - $\pi^*$	BD (2) C16 - C17	1.633	BD*(2) C14 - O15	0.277	65.98	0.3	0.06
			BD*(2) C18 - C21	0.277	89.54	0.29	0.07
			BD*(2) N19 - C23	0.366	69.71	0.27	0.06
$\pi$ - $\pi^*$	BD (2) C18 - C21	1.636	BD*(2) C16 - C17	0.335	74.85	0.28	0.06
			BD*(2) N19 - C23	0.366	122.13	0.27	0.08
$\pi$ - $\pi^*$	BD (2) N19 - C23	1.706	BD*(2) C16 - C17	0.335	112.97	0.32	0.08
			BD*(2) C18 - C21	0.277	52.59	0.33	0.06
n - $\pi^*$	LP (2) S1	1.622	BD*(2) C2 - C3	0.351	87.15	0.27	0.07
			BD*(2) C4 - C5	0.309	91.55	0.26	0.07
n - $\pi^*$	LP (2) N12	1.667	BD*(2) C9 - N11	0.209	115.14	0.29	0.08
			BD*(2) C14 - O15	0.017	4.44	0.88	0.03
			BD*(2) C14 - O15	0.277	190.41	0.32	0.11
n - $\sigma^*$	LP (1) O15	1.855	BD*(1) N12 - C14	0.084	118.2	0.67	0.12
			BD*(1) C14 - C16	0.069	80.37	0.66	0.10
n - $\sigma^*$	LP (1) N19	1.916	BD*(1) C16 - C17	0.033	39.33	0.90	0.08

**Table 5** The frontier molecular orbital of T<sub>2</sub>CNH.

Occupancy	Orbital energies (a.u)	Orbital energies (eV)	Kinetic energies (a.u)
O <sub>56</sub>	-0.292	-7.947	1.641
O <sub>57</sub>	-0.284	-7.740	1.641
O <sub>58</sub>	-0.271	-7.390	1.582
O <sub>59</sub>	-0.269	-7.342	2.186
O <sub>60</sub>	-0.229	-6.248	1.567
V <sub>61</sub>	-0.081	-2.223	1.590
V <sub>62</sub>	-0.055	-1.503	1.586
V <sub>63</sub>	-0.055	-1.503	1.424
V <sub>64</sub>	-0.019	-0.519	0.488
V <sub>65</sub>	-0.009	-0.255	0.535

**Table 6** The Physico-Chemical properties of T<sub>2</sub>CNH.

Parameters	Values
HOMO	-6.248 eV
LUMO	-2.223 eV
Energy gap	4.025 eV
Ionization potential (IP)	6.248 eV
Electron affinity (EA)	2.223 eV
Electrophilicity Index ( $\omega$ )	2.562
Chemical Potential ( $\mu$ )	7.359
Electro negativity ( $\chi$ )	-7.359
Hardness ( $\eta$ )	-4.025

286 nm which correlates well with the experimental values 340 and 290 nm. The more intense band at 340 nm has maximum oscillator strength ( $f=0.6909$ ), corresponds to Homo-Lumo transition and is mostly characterized as n- $\pi^*$  type. This type of transition is attributed to the presence of large no of free lone pairs of electrons available on sulphur (S<sub>1</sub>), Nitrogen (N<sub>11</sub>, N<sub>12</sub>) and oxygen (O<sub>15</sub>) atoms. The experimental and theoretical UV-Vis absorption spectrum is shown in **Figure 5**. The density of states spectrum of T<sub>2</sub>CNH is shown in **Figure 6**. It was used to calculate group contributions to the molecular orbitals (HOMO and LUMO). DOS plot shows population analysis per orbital and demonstrates a simple view of the character of the molecular orbitals (MOs) in a certain energy range.

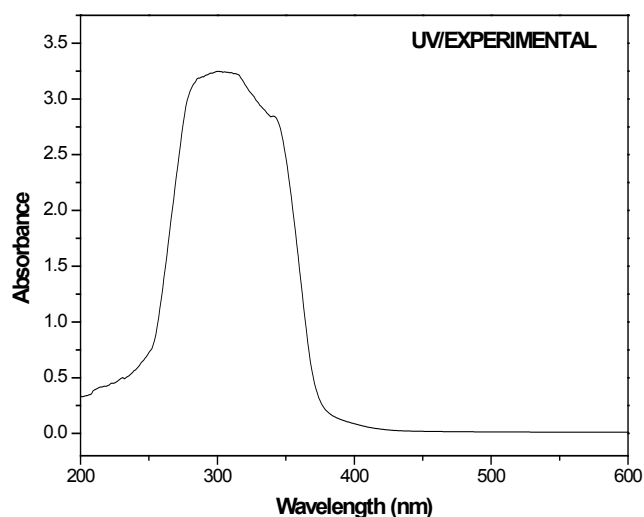
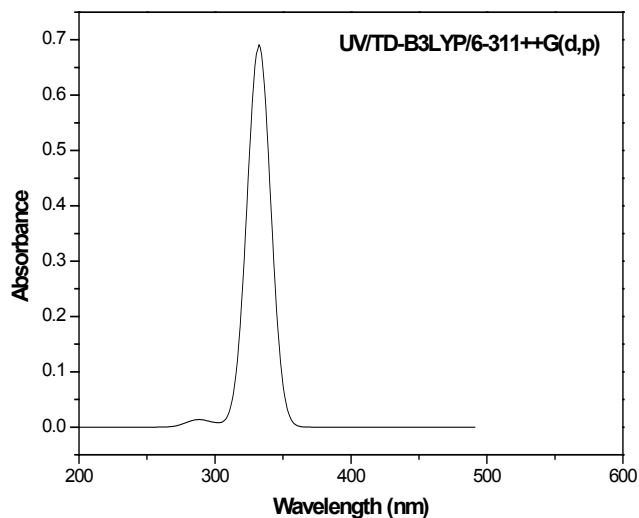


**Figure 5** The Theoretical and Experimental UV-Visible spectra of  $T_2CNH$ .

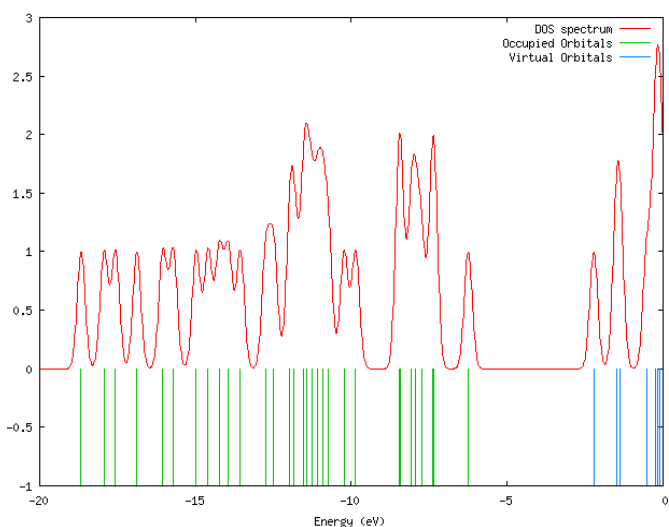


**Figure 6** The DOS spectrum of  $T_2CNH$ .

## MEP Analysis

The molecular electrostatic potential (MEP) is widely used as a reactivity map displaying most probable regions for the electrophilic attack of charged part on organic molecule. MEP plot provides a simple way in predicting the interaction of different geometries. In order to predict the reactive sites for electrophilic and nucleophilic attacks of the  $T_2CNH$ , MEP was calculated with DFT/B3LYP/6-311++G(d,p) level of theory. The negative (red color) and positive (blue color) regions of MEP are related to electrophilic and nucleophilic reactivity respectively is shown in **Figure 7**. The negative region is located over the carbonyl group and the positive region is located over Hydrogen atom in the hydrazone linkage.

## Mulliken Charges Analysis

The Mulliken atomic charge calculation has an important role in the application of quantum chemical calculation to molecular system, because the atomic charges should affect dipole moment, polarizability, electronic structure and more a lot of properties of molecular systems. The total atomic charges of  $T_2CNH$  are calculated by Mulliken population analysis with B3LYP/6-311++G(d,p) basis set and its values are listed in **Table 8**. The Mulliken atomic charge plot for  $T_2CNH$  is shown in **Figure 8**. The  $C_9/C_3$

**Table 7** The electronic transition of  $T_2CNH$ .

Calculated at B3LYP/6-311++G(d,p)	Oscillator strength	Calculated Band gap (eV/nm)	Experimental Band gap (nm)	Type
Excited State 1	Singlet-A (f=0.6909)	3.7311 eV/332.30 nm	340	$\pi-\pi^*$
60 -> 61	0.6388	-4.0254		
60 -> 62	0.1325	-4.7451		
Excited State 2	Singlet-A (f=0.0043)	4.1118 eV/301.54 nm		
59 -> 61	0.6467	-5.1187		
59 -> 62	0.1819	-5.8384		
Excited State 3	Singlet-A (f=0.0126)	4.3234 eV/286.77 nm	290	$\pi-\pi^*$
60 -> 62	0.4175	-4.7451		
60 -> 63	0.5580	-4.8692		

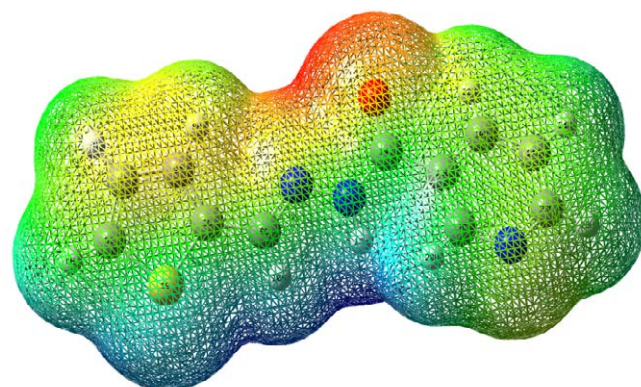


**Figure 7** Molecular electrostatic potential map of  $T_2CNH$ .

atoms have the highest negative/positive charges, respectively among the other atoms in T<sub>2</sub>CNH due to the resonance.

## Thermodynamical Properties

Several thermodynamic parameters have been calculated using DFT/B3LYP/6-311++G(d,p) basis set are listed in **Table 9**. The thermodynamic parameters viz, entropy ( $S_m^0$ ), enthalpy ( $\Delta H_m^0$ ) and heat capacity at constant pressure ( $C_{p,m}^0$ ) for T<sub>2</sub>CNH was calculated from the theoretical harmonic wavenumbers obtained from B3LYP/6-311++G(d,p) basis set in the range 100-1000 k and listed in **Table 10**. It is evident from the **Table 10** that the thermodynamic parameters increase with rise of temperature

**Table 8** The Mulliken atomic charges of T<sub>2</sub>CNH.

Atoms	Charges	Atoms	Charges	Atoms	Charges
S1	-0.6516	H10	0.1263	N19	-0.0124
C2	0.2759	N11	0.1794	H20	0.1758
C3	1.9917	N12	-0.0550	C21	-0.0964
C4	-1.2036	H13	0.2477	H22	0.2280
C5	0.4451	C14	-0.7857	C23	-0.3517
H6	0.2687	O15	-0.2925	H24	0.1897
H7	0.1582	C16	0.9920	H25	0.1903
H8	0.2452	C17	-0.5899		
C9	-1.7721	C18	0.0967		

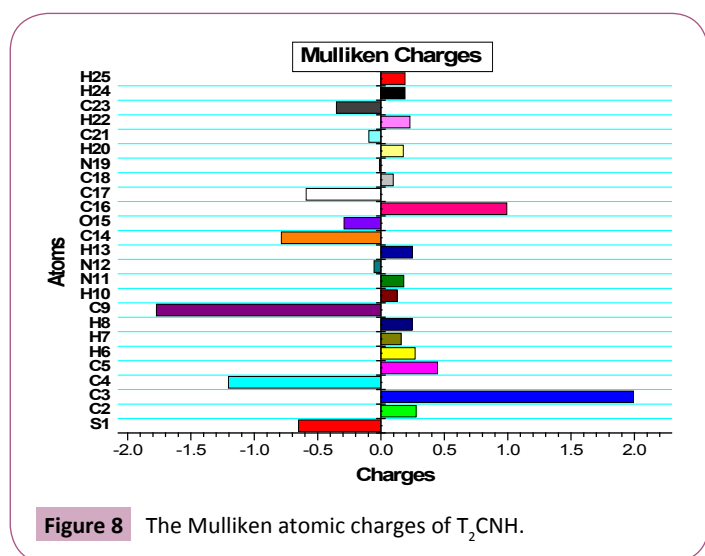


**Figure 8** The Mulliken atomic charges of T<sub>2</sub>CNH.

**Table 9** The calculated total energy (a.u), zero point vibrational energies (kcal/mol), rotational constants (GHZ) and entropy (cal/mol K<sup>-1</sup>) for T<sub>2</sub>CNH.

Parameters	B3LYP/6-311++G(d,p)
Total Energies	-1062.41677
Zero-point Energy	114.99338 (Kcal/Mol)
Rotational constants (GHZ)	1.78813
	0.15572
	0.14465
Entropy	
Total	122.336
Translational	42.214
Rotational	33.345
Vibrational	46.777

due to the fact that the molecular vibrational intensities increase with temperature. The correlation equations between these thermodynamic parameters and temperature were fitted by parabolic formula and the regression coefficient is also given in the parabolic equation. The correlation relation between the thermodynamic parameters and temperature are as follows:

$$C_{p,m}^0 = 4.44266 + 0.01876T + 1.6571 \times 10^{-5} T^2 \quad (R^2=0.99929)$$

$$S_m^0 = 1.35549 + 0.00572T + 5.0560 \times 10^{-5} T^2 \quad (R^2=0.99997)$$

$$\Delta H_m^0 = 3.15466 + 0.01332T + 1.1767 \times 10^{-5} T^2 \quad (R^2=0.99944)$$

The correlation graphs between various thermodynamic functions and temperature are graphically presented in **Figure 9**.

## Conclusion

The complete vibrational analysis has been performed to using quantum chemical calculation at DFT method for the first time to the title molecule T<sub>2</sub>CNH. The calculated bond parameters are good agreement with the related single crystal X-ray diffraction (XRD) data. In T<sub>2</sub>CNH, the thiophene and hydrazone moieties are co-planar, which shows a good conjunction between p-orbitals of all atoms of thiophene and hydrazone moieties. The vibrational

**Table 10** Thermodynamic properties of T<sub>2</sub>CNH at different temperatures.

T (K)	S (Jmol <sup>-1</sup> K <sup>-1</sup> )	Cp (Jmol <sup>-1</sup> K <sup>-1</sup> )	ddH (kJmol <sup>-1</sup> )
100	349.07	100	6.95
200	436.15	159.71	19.86
298.15	511.96	224.53	38.7
300	513.36	225.74	39.12
400	586.95	287.34	64.85
500	656.77	338.54	96.24
600	722.24	379.34	132.21
700	783.25	411.8	171.83
800	840.01	438.01	214.36
900	892.88	459.52	259.27
1000	942.25	477.43	306.15

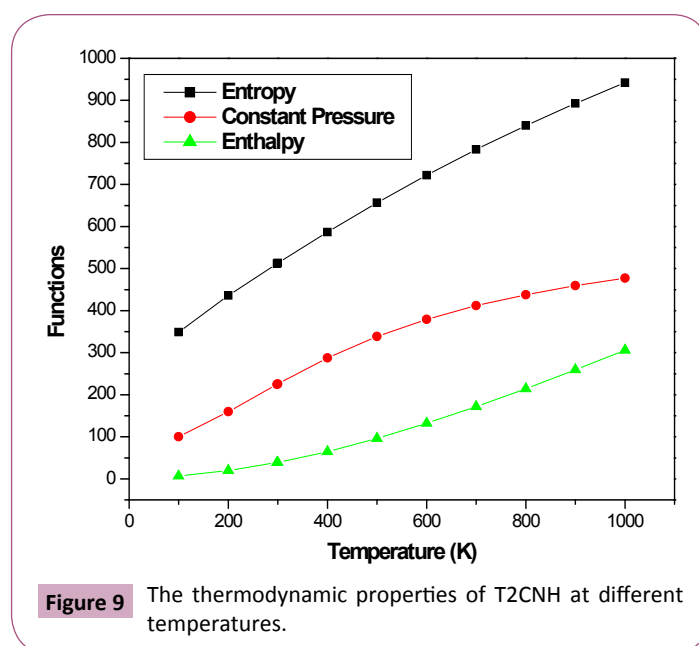


**Figure 9** The thermodynamic properties of T<sub>2</sub>CNH at different temperatures.

data of T<sub>2</sub>CNH are well supported by the harmonic and related literature values. The  $\beta_0$  value of T<sub>2</sub>CNH molecule is found to be  $1.5861 \times 10^{-30}$  esu, which is four time greater than that of urea. The NBO result reflects the charge transfer within the molecule and the maximum energy takes place during  $\pi$ - $\pi^*$  transition. The Homo-Lumo band gap was calculated about 4.025 eV, which

leads the T<sub>2</sub>CNH molecule to become less stable and more reactive. The recorded UV-Vis spectral values agree well with calculated values. MEP surface predicts the reactive sites for electrophilic and nucleophilic attack. In addition, Mulliken atomic charges, zero point energy and thermodynamic properties are also calculated.



## References

- 1 The Encyclopædia Britannica (1882), Nature 25: 313-315.
- 2 Molvi KI, Vasu KK, Yerande SG, Sudarsanam V, Haque N (2007) Syntheses of new tetrasubstituted thiophenes as novel anti-inflammatory agents. *Euro J Medi Chem* 42: 1049-1058.
- 3 Rai NS, Kalluraya B, Lingappa B, Shenoy S, Puranic VG (2008) Convenient access to 1,3,4-trisubstituted pyrazoles carrying 5-nitrothiophene moiety via 1,3-dipolar cycloaddition of sydnone with acetylenic ketones and their antimicrobial evaluation. *Euro J Medi Chem* 43: 1751-1720.
- 4 Ashalatha BV, Narayana B, Raj KKV, Kumari NS (2008) Synthesis of some new bioactive 3-amino-2-mercapto-5,6,7,8-tetrahydro[1]benzothieno[2,3-d]pyrimidin-4(3H)-one derivatives. *Euro J Medi Chem* 42: 719-728.
- 5 Polivka Z, Holubek J, Svatek E, Metys J, Protiva M (1984) Potential hypnotics and anxiolytics: Synthesis of 2-bromo-4-(2-chlorophenyl)-9-[4-(2-methoxyethyl)piperazino]-6H-thieno[3,2,4-triazolo[4,3-a]-1,4-diazepine and of some related compounds. *Collect Czech Chem Commun* 49: 621-623.
- 6 Noguchi H, Kitazumi K, Mori M, Shiba T (2004) Electroencephalographic Properties of Zaleplon, a Non-Benzodiazepine Sedative/Hypnotic, in Rats. *J Pharm Sci* 94: 246-251.
- 7 Kim S, Yoon JY (2004) Hydrazones in science and synthesis. *Sci Synth* 27: 671-722.
- 8 Brehme R, Enders D, Fernandez R, Lassaletta JM, Aldehyde N (2007) N-Dialkylhydrazones as Neutral Acyl Anion Equivalents: Umpolung of the Imine Reactivity. *Eur J Org Chem* 34: 5629-5660.
- 9 Belskaya NP, Dehaen W, Bakulev VA (2010) Synthesis and properties of hydrazones bearing amide, thioamide and amidine functions. *Archive Org Chem* 275-332.
- 10 Bhole RP, Bhusari KP (2009) Synthesis, antimycobacterial activity and 3-d qsar studies of some new derivatives of p-hydroxybenzohydrazide. *QSAR Comb Sci* 28: 1405-1417.
- 11 Loncle C, Brunel JM, Vidal N, Dherbomez M, Letourneux Y (2004) Synthesis and antifungal activity of cholesterol-hydrazone derivatives. *Eur J Med Chem* 39: 1067-1071.
- 12 KK Bedia, Elcin O, Seda U, Fatma K, Nathaly S (2006) Synthesis and characterization of novel hydrazide-hydrazones and the study of their structure-antituberculosis activity. *Eur J Med Chem* 41: 1253-1261.
- 13 Subashchandrabose S, Meganathan C, Erdogdu Y, Saleem H, Jayakumar C (2013) Vibrational and conformational analysis on N1-N2-bis(pyridine-4-yl)methylene)benzene-1, 2-diamine. *J Mol Struct* 1042: 37-44.
- 14 Subramanian N, Sundaraganesan N, Jayabharathi JA (2010) Molecular structure, spectroscopic (FT-IR, FT-Raman, NMR, UV) studies and first order molecular hyperpolarizabilities of 1,2-bis(3-methoxy-4-hydroxy benzlidene) hydrazine by density functional method. *Spectrochim Acta A Mol Biomol Spectrosc* 76: 259-269.
- 15 Frisch MJ, Trucks GW, Schlegel HB, Scuseria GE, Robb MA, et al. (2004) Theoretical and Computational Aspects of Magnetic Organic Molecules. Gaussian Inc, Wallingford, CT.
- 16 Schlegel HB (1982) Optimization of equilibrium geometries and transition structures. *J Comput Chem* 3: 214-218.
- 17 Jamróz MH (2006) Vibrational modes of 2,6-, 2,7-, and 2,3-diisopropyl-naphthalene, A DFT study. *J Mol Struct* 787: 172-183.
- 18 Michalska D (2003) Raint Program, Wroclaw University of Technology, Poland.
- 19 Michalska D, Wysokinski R (2005) The prediction of Raman spectra of platinum(II) anticancer drugs by density functional theory. *Chem Phys Lett* 403: 211-217.
- 20 Fleming GD, Koch R, Vallete MMC (2006) Theoretical study of the syn and anti thiophene-2-aldehyde conformers using density functional theory and normal coordinate analysis. *Spectrochim Acta A Mol Biomol Spectrosc* 65: 935-945.
- 21 Balachandran V, Janaki A, Nataraj A (2014) Theoretical investigations on molecular structure, vibrational spectra, HOMO, LUMO, NBO analysis and hyperpolarizability calculations of thiophene-2-carbohydrazide. *Spectrochim Acta A Mol Biomol Spectrosc* 118: 321-330.
- 22 Unal A, Eren B (2013) FT-IR, dispersive Raman, NMR, DFT and antimicrobial activity studies on 2-(Thiophen-2-yl)-1H-benzo[d]imidazole. *Spectrochim Acta A Mol Biomol Spectrosc* 114: 129-136.
- 23 Brathen O, Kveseth K, Nielsen CJ, Hagen K (1986) Molecular structure and conformational equilibrium of gaseous thiophene-2-aldehyde as studied by electron diffraction and microwave, infrared, Raman and matrix isolation spectroscopy. *J Mol Struct* 145: 45-68.
- 24 Geiger DK, Geiger HC, Williams L, Noll BC (2012) 2-(Thiophen-2-yl)-1-(thiophen-2-ylmethyl)-1 H -benzimidazole. *Acta Cryst E: Structure Reports Online* 68: o420.
- 25 Rauhut G, Pulay P (1995) Transferable Scaling Factors for Density Functional Derived Vibrational Force Fields. *J Phys Chem* 99: 3093-3100.
- 26 Bellamy LJ (1980) The infrared spectra of complex molecules, vol 2 champman and Hall, London.
- 27 Babu NR, Subashchandrabose S, Padusha MSA, Saleem H, Manivannan V, et al. (2014) Synthesis and structural characterization of (E)-N'-((Pyridin-2-yl) methylene) benzohydrazide by X-ray diffraction, FT-IR, FT-Raman and DFT methods. *J Mol Struct* 1072: 84-93.
- 28 Varsanyi G (1974) Assignments of vibrational spectra of 700 Benzene Derivatives, Wiley, New York.
- 29 Sathyanarayanan DN (2000) Vibrational spectroscopy theory and Applications, 446-447.
- 30 Varsanyi G (1973) Assignments for Vibrational Spectra of Seven Hundred Benzene derivatives, 1/2 Academic Kiado.
- 31 Jag M (2001) Organic Spectroscopy Principles and Application, (2nd edn), Narosa Publishing house, New Delhi.
- 32 Lorenc J (2012) Dimeric structure and hydrogen bonds in 2-N-ethylamino-5-methyl-4-nitro-pyridine studied by XRD, IR and Raman methods and DFT calculations. *Vib Spectrosc* 61: 112-123.
- 33 Krishnakumar V, Dheivamalar S, Xavier RJ, Balachandran V (2006) Analysis of vibrational spectra of 4-amino-2, 6-dichloropyridine and 2-chloro-3, 5-dinitropyridine based on density functional theory calculations. *Spectrochim Acta A Mol Biomol Spectrosc* 65: 147-154.
- 34 Sundaraganesan N, Saleem H, Mohan S (2003) Vibrational spectra, assignments and normal coordinate analysis of 2-amino-5-bromopyridine. *Spectrochim Acta A Mol Biomol Spectrosc* 59: 1113-1118.
- 35 Silverstein M, Basseller CG, Morill C (1981) Spectrometric identification of organic compound, Wiley; \.

- 36 Badawi HM (2009) Structural stability, C–N internal rotations and vibrational spectral analysis of non-planar phenylurea and phenylthiourea. *Spectrochim Acta A Mol Biomol Spectrosc* 72: 523-527.
- 37 James C, Ravikumar C, Sundius T, Krishnakumar V, Kesavamoorthy R, et al. (2008) FT-Raman and FTIR spectra, normal coordinate analysis and ab initio computations of (2-methylphenoxy) acetic acid dimer. *Vib Spectrosc* 47: 10-20.
- 38 Weinhold F, Landis CR (2005) *Valency and bonding: a natural bond orbital donor-acceptor perspective*. Cambridge University Press.
- 39 Ott JB, Boerio-Goates J (2000) *Calculations from Statistical Thermodynamics*.